Proceedings of the ASME 2010 3rd Joint US-European Fluids Engineering Summer Meeting and 8th International Conference on Nanochannels, Microchannels, and Minichannels
FEDSM-ICNMM2010
August 1-5, 2010, Montreal, Canada

FEDSM-ICNMM2010-30798

Investigation of streaming flow patterns in a thermoacoustic device using PIV

Hadi Babaei
Department of Mechanical and Materials Engineering, University of Western Ontario, London, ON, Canada, N6A 5B9

Kamran Siddiqui
Department of Mechanical and Materials Engineering, University of Western Ontario, London, ON, Canada, N6A 5B9

ABSTRACT

We report on an experimental study conducted to study the streaming velocity fields in the vicinity of the stack in a thermoacoustic device. Synchronized Particle Image Velocimetry (PIV) technique was used to measure the two-dimensional streaming velocity fields. The streaming velocity fields were measured at both sides of the porous stack over a range of pressure amplitudes (drive ratios). The results show that the streaming flow structure is significantly different on hot and cold sides of the stack. The hot side of the stack experienced higher magnitudes and higher spatial variability of the streaming velocities compared to the cold side. The difference in the velocity magnitude between the hot and cold sides of the stack showed a significant increase with an increase in the drive ratio.

INTRODUCTION

Streaming is referred to as a second-order mass-flux density or velocity which is driven by and superimposed on the larger first-order oscillating acoustic velocity [1]. Streaming flow that originates within the viscous boundary layer of the wall and affects the entire tube is called boundary layer-driven streaming [1]. Boundary layer-driven streaming is important in standing-wave thermoacoustic heat engines and refrigerators. The classical theory classifies this type of streaming into (i) Rayleigh or outer streaming, and (ii) Schlichting or inner streaming. Outer streaming corresponds to the mean fluid motion outside the boundary layer and inner streaming corresponds to the mean fluid motion inside the boundary layer [1]. The classical theory predicts two streaming vortices per quarter-wavelength of the acoustic wave symmetrical about the center line of the resonator. This streaming flow pattern is referred to as regular, slow or linear streaming, despite the fact that even slow streaming is a result of nonlinear phenomenon. As the acoustic pressure amplitude increases the streaming velocity deviates from slow streaming. When the shape and number of streaming vortices become distorted from the classical one, irregular (fast or nonlinear) streaming pattern is formed [1, 2].

Few studies have investigated the impact of the transverse temperature gradient on the streaming flow pattern in a resonator tube. For example, Nabavi *et al.* [3] experimentally investigated the effect of transverse temperature gradient on the streaming patterns. They observed that the temperature difference as low as 0.8 ˚C between the top and bottom walls could distort the two streaming vortices symmetric about the channel centerline obtained at the isothermal condition to a single vortex.
Thompson *et al.* [4] found that the axial temperature gradient also influences the streaming flow pattern. They observed that the streaming field became irregular even in the presence of small temperature gradients.

Thermoacoustics is a new and emerging branch of science that deals with the interaction of heat and sound. Thermoacoustic engine deals with the conversion of heat into sound whereas, thermoacoustic refrigerator deals with the conversion of sound into heat. A thermoacoustic refrigerator consists of a resonance tube, a stack, two heat exchangers and an acoustic source, such as a loudspeaker, to excite acoustic standing wave in the tube. Stack, which is the heart of a thermoacoustic device, could be in the form of parallel plates, pin array or a porous medium. The two heat exchangers maintain the desired temperature gradient across the stack by transferring heat to and from the thermal reservoirs located outside the device. To understand the basic thermoacoustic phenomenon, a simplified configuration of the thermoacoustic refrigerator is used which is comprised of a resonance tube, a stack and an acoustic source (i.e. without heat exchangers) [5]. In such a configuration the stack is also termed as a thermoacoustic couple.

Characterization of the flow field in around a thermoacoustic stack is an essential step to understand and optimize heat exchange among the stack, heat exchanger and working gas in a thermoacoustic device. Several studies investigated the velocity field in and around the stack in a thermoacoustic couple.

Blanc-Benon *et al.* [6] experimentally and computationally visualized the flow field in the vicinity of the cold end of the stack. Particle image velocimetry (PIV) technique was used for the experimental measurements. They observed that the flow at the edges of the stack plates is influenced by the plate thickness. They found concentric vortices off the edge of the thicker plates, whereas, the vorticity layers are elongated off the edge of the thinner plates.

Mao *et al.* [7] used PIV to study the flow dynamics at the stack edge over different phases of an acoustic cycle. They found that the vortex dynamics changes with the phase of the acoustic excitation cycle due to the ejection and suction of the flow at the stack edge. They also observed that the shape of the vortices is also influenced by the Reynolds number at a particular phase. Their pattern changed from elongated to concentric with an increase in the Reynolds number. They also found that the vortex structures changes with a change in the plate thickness.

Jaworski *et al.* [8] also studied the flow behavior at the edge of a parallel plate stack as a function of the acoustic excitation cycle phase using PIV. They also observed changes in the flow structure in the vicinity of the stack plates with the phase.

Recently, Aben *et al.* [9] studied the flow in the vicinity of the parallel-plate stack using PIV. They also observed changes in the pattern of vortices off the edge of the stack plate with a change in the phase, plate edge geometry and the plate thickness. They argued that the Reynolds and Strouhal numbers are the appropriate dimensionless parameters to classify different patterns of vortices. They have also measured the streaming velocity field in the vicinity of the stack plates which comprised of a pair of counter rotating vortices at the plate edge.

Streaming is important in thermoacoustic heat engines and refrigerators since it is a mechanism for convective heat transfer. This heat transfer could be an undesirable process which may decrease the efficiency of thermoacoustic devices. Therefore, understanding of the streaming velocity field in a thermoacoustic device and its control are vital to achieve higher efficiency for these devices.

Except for Aben *et al.* [9] who presented preliminary results of the streaming velocity field in the vicinity of a thermoacoustic stack, all other above-mentioned studies considered the oscillating acoustic velocity field. Furthermore, all of these studies were focused on one end of the stack. As the temperature at the two ends of the stack is substantially different, the streaming flow structure is expected to vary at the two ends as the streaming flow pattern is very sensitive to the temperature gradients [3, 4].

Present study is focused on investigating the streaming velocity field on both sides of the stack using synchronized Particle Image Velocimetry (PIV) technique.

EXPERIMENTAL SETUP

The experiments were conducted in a Plexiglas resonator tube, 121 cm in length with the inner cross sectional area of 11.5 cm × 11.5 cm. The thickness of the Plexiglas sheets was 1.1 cm which held the rigid wall assumption. The resonator was filled with air at atmospheric pressure. To excite a half wavelength acoustic standing wave in the tube, a 200 W loudspeaker (PR 65 NEO) was used. A function generator (Agilent 33120A) was used to generate sinusoidal waves of different amplitudes at the frequency of 146 Hz. The accuracy of the amplitude and frequency were ±0.1 mV and ±1 μHz, respectively. A 220 W amplifier, (Pioneer SA-1270) was used to amplify the output signal of the function generator. The amplified signal was used to feed the loudspeaker. A microphone model 377A10 PCB Piezotronics was used to monitor the acoustic pressure. The open circuit sensitivity of the microphone is 1.94 mV/Pa at 251.2 Hz. The frequency response of the microphone is nearly flat between 20 and 1000 Hz. The microphone was placed in a drilled hole at the closed end of the tube. The microphone was connected to an oscilloscope which was used to monitor and record the wave characteristics including frequency and pressure amplitude. The experimental setup used in this study is shown schematically in figure 1 (a).

For the PIV measurements, a 120 mJ Nd:YAG laser (SoloPIV 120XT) was used as a light source. A CCD camera (JAI CV-M2) was used to capture the images via a frame grabber card (DVR Express) that acquired 8 bit images at a rate of 30 Hz. The resolution of the camera was 1600 × 1200 pixels. Bis (2-ethylhexyl) sebacate mist having an average diameter of 0.5 μm was employed as the tracer particles. Mist was produced by an aerosol generator (Lavision Inc., Ypsilanti MI). The experiments were conducted in the presence of a porous RVC stack that has on average 20 pores per inch. The stack was 3.1 cm in length and has cross-sectional area almost the same as the resonator.

The camera field of view was set equal to 8.6 cm in the direction of the acoustic wave propagation and 11.5 cm perpendicular to the acoustic wave propagation. Figure 1(b) shows the top view of the schematic. The stack was placed at the center of the camera field of view which corresponds to the normalized stack center position of x_{cn} = 0.22. This stack location was within the optimum range that a stack should be placed in a thermoacoustic device. The experiments were conducted at the frequency of 146 Hz at seven different pressure amplitudes of the acoustic standing wave ranging from 200 Pa to 950 Pa. The corresponding drive ratios are 0.2% to 0.94%, respectively.

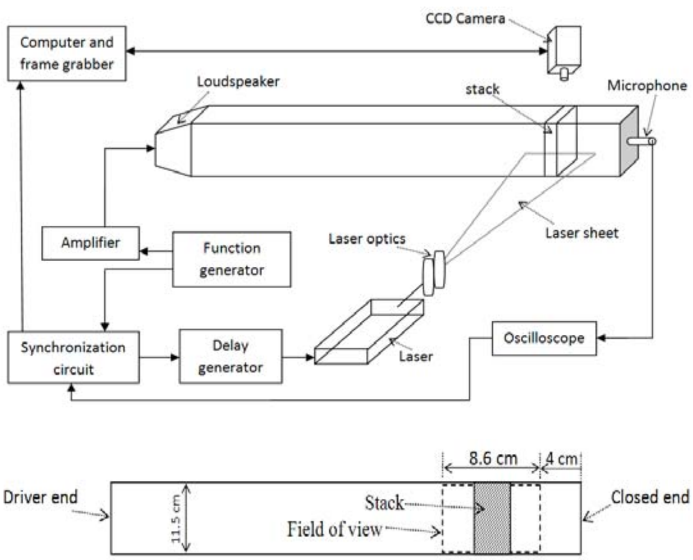

Figure 1: (Top) Schematic of the experimental set-up, (Bottom) top view of the resonator showing the stack (shaded region) and the field of view of the camera (dashed lines)

To be able to capture the streaming velocity fields, the two laser pulses must shine exactly at the same phase of the acoustic wave. A synchronized PIV technique reported by Nabavi *et al.* [3] was used in the present study to capture the streaming velocity fields. To synchronize the PIV system (laser and camera) with a specified acoustic wave phase, the wave excitation signal was used to trigger the camera and the laser through a synchronization circuit [10]. The size of interrogation and search regions was set equal to 32 × 32 pixels and 64 × 64 pixels for the PIV cross-correlation, respectively. The nominal resolution of the velocity field was increased to 16 × 16 pixels by using a 50% overlap window. The correlation peak with sub-pixel accuracy was obtained by using a three-point Gaussian sub pixel fit scheme. 200 PIV images were captured for each set of measurements and, therefore, 100 streaming velocity fields were acquired. The uncertainty in the velocity was estimated to be less than ±0.153 cm/s.

RESULTS AND DISCUSSION

Instantaneous streaming velocity fields at both ends of the stack at low and high drive ratios (0.44%, 0.93%) are shown in figure 2 (a) and (b), respectively. The upper stack edge (upper dashed line in the figure) in the plots corresponds to the cold end of the stack and the lower stack edge (lower dashed line) corresponds to the hot end of the stack.

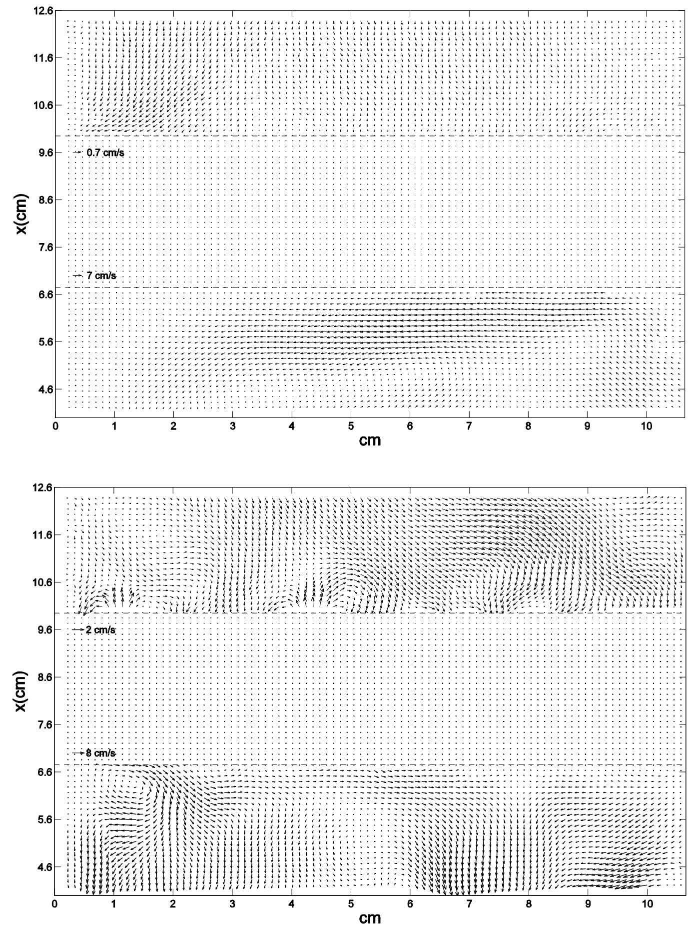

Figure 2: Instantaneous streaming velocity fields on both sides of the stack at the drive ratio of (top) 0.44% and (bottom) 0.93%. The dashed-lines indicate the stack edges.

The velocity fields show that the stack separated the streaming flow into two regions on either sides of the stack and the flow structure appeared to be disconnected from each other. Another interesting feature observed in figure 2 was that the magnitudes of streaming velocities on either sides of the stack were different. The streaming velocity field close to the hot end of the stack was higher in magnitude as compared to the streaming velocity field closer to the cold end of the stack. The higher velocity magnitude in the hot-end region was likely due to the superposition of the convective motions due to the high temperature gradients, on the streaming flow.

The above velocity vector plots provide a good perception about the streaming flow structure on both sides of a porous stack. It also provides a good understanding of the flow scales, relative velocity magnitudes and how the drive ratio alters the flow structure. A quantitative analysis of the flow characteristics under different conditions was conducted to quantify the influence of these conditions on the streaming flow field.

The spatial variations in the streaming velocity fields were quantified in terms of the standard deviation of the spatial velocity field for both *u*- and *v*-components of velocity computed separately in the hot-end and cold-end regions. For each case, the standard deviations were computed in each velocity field and then averaged over all velocity fields. The standard deviations of *u* and *v* velocity components on both sides of the stack are shown in figure 3 and figure 4, respectively.

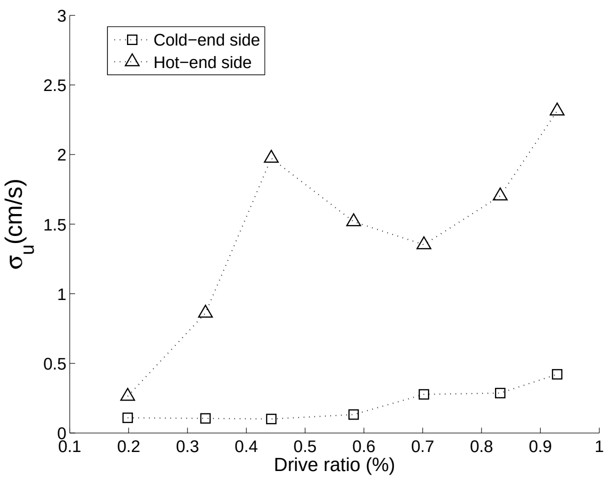

Figure 3: The spatial variation of the *u* component of the streaming velocity on hot and cold sides of the stack for different drive ratios.

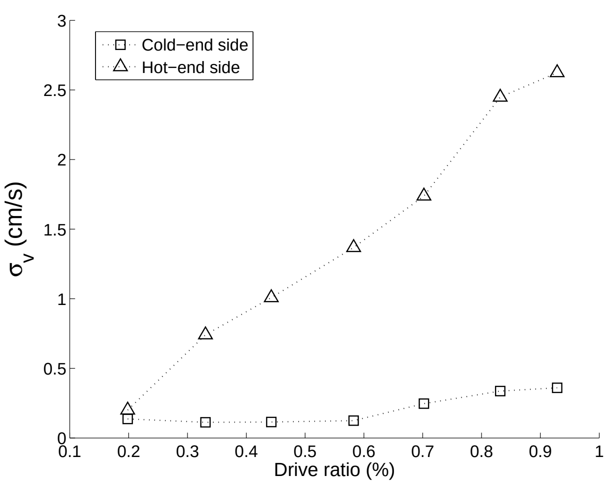

Figure 4: The spatial variation of the *v* component of the streaming velocity on hot and cold sides of the stack for different drive ratios.

The results in figures 3 and 4 clearly show that the streaming velocity field on the hot side of the stack has significantly high spatial variability than that on the cold side of the stack. Results also show that at the lowest drive ratio, the spatial variability is very low and is almost identical on hot and cold sides of the stack. However, with an increase in the drive ratio, the variability on the cold side does not increase considerably. However, the spatial variability on the hot side increases significantly with an increase in the drive ratio. Comparison of figures 3 and 4 show that on the cold side, the spatial variability of both *u* and *v* velocity components is almost identical. On the hot side, the spatial variability of the *v* velocity component is slightly higher than the *u* velocity component at the higher drive ratios.

The plots in figures 3 and 4 quantify the spatial variability of the streaming velocity fields but they do not quantify the magnitudes of the streaming velocity field for different drive ratios. The magnitudes of the streaming velocity fields are quantified in terms of the root-mean-square of the resultant velocity field (V_{rms}). The values of V_{rms} on both sides of the stack are shown in figure 5. The plot shows that the streaming velocity magnitude increases with the drive ratio on both sides of the stack. However, the increase in velocity magnitude on the hot side is more substantial. The results show that as the drive ratio increased from 0.2% to 0.93%, the velocity magnitude on the cold side increased by almost a factor of three while, the velocity magnitude on the hot side increased by more than a factor of seven.

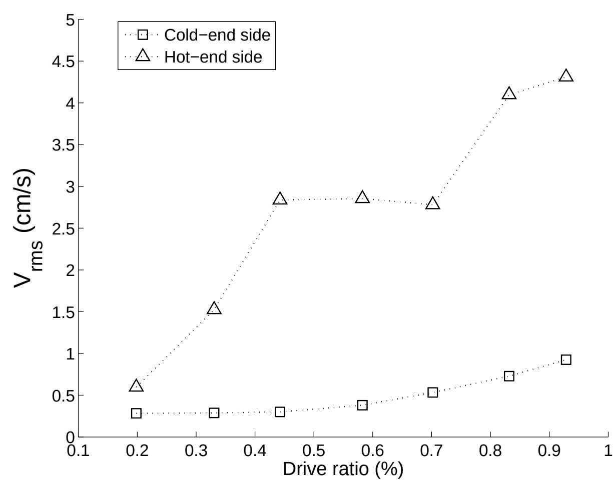

Figure 5: RMS streaming velocity magnitude on hot and cold sides of the stack for different drive ratios.

CONCLUSION

The acoustic streaming influences the heat transfer in a thermoacoustic device, which could affect the overall performance of the device. The structure of acoustic streaming in the presence of thermoacoustic stacks needs to be investigated to address the challenges associated with this phenomenon. In the present study, the streaming flow field in a thermoacoustic device was investigated using synchronized PIV technique. RVC was chosen as the thermoacoustic stack. The experiments were performed at seven different drive ratios raging from 0.2% to 0.94%. The experiments not only demonstrated the complexity of streaming patterns but also showed the huge influence of the presence of the porous stack on the structure of the streaming velocity field. The magnitude of streaming velocity components was larger on the hot side of the stack compared to the cold side at all drive ratios under investigation. An increase in the drive ratio not only made the streaming pattern more complex but also widened the difference in the steaming velocity magnitude on the hot and cold sides. The present experiments confirm the complex interaction of the streaming velocity field with the stack. Further detailed investigation on acoustic streaming is needed for the better understanding of this phenomenon and to enhance the performance of thermoacoustic devices.

REFERENCES

[1] Boluriaan, S., Morris, P.J., “Acoustic streaming: from Rayleigh to today”, *aeroacoustics*, 2, 255-292, 2003.

[2] Nabavi, M., Siddiqui, K. and Dargahi, J., “Analysis of regular and irregular acoustic streaming patterns in a rectangular enclosure”, *wave motion*, 46, 312-322, 2009.

[3] Nabavi, M., Siddiqui, K. and Dargahi, J., “Effects of transverse temperature gradient on acoustic and streaming velocity fields in a resonant cavity”, *Applied Physics Letter*, 93, 051902, 2008.

[4] Thompson, M. W. and Atchley, A. A. and Maccarone, M.J., “Influences of a temperature gradient and fluid inertia on acoustic streaming in a standing wave”, *J. Acoust. Soc Am*, 117, 1839-1849, 2005.

[5] Wheatley J., Hofler T., Swift G.W., and Migliori A., “An intrinsically irreversible thermoacoustic heat engine”, *J. Acoust. Soc. Am.* 74, 153-170, 1983.

[6] Blanc-Benon P., Besnoin E., Knio O., “Experimental and computational visualization of the flow field in a thermoacoustic stack”, *C.R. Mecanique* 331, 17-24, 2003.

[7] Mao X., Yu Z., Jaworski A.J., Marx D., “PIV studies of coherent structures generated at the end of a stack of parallel plates in a standing wave acoustic field”, *Exp Fluids* 45, 833-846, 2008.

[8] Jaworski A.J., Mao Xi., Mao Xu., Yu Z., “Entrance effects in the channels of the parallel plate stack in oscillatory flow conditions”, *Experimental Thermal and Fluid Science* 33, 495-502, 2009.

[9] Aben P.C.H., Bloemen P. R., Zeegers J. C. H., “2-D measurements of oscillatory flow around parallel plates”, *Exp Fluids* 46, 631-641, 2009.

[10] Nabavi, M., Siddiqui, K. and Dargahi, J., “Simultaneous measurements of acoustic and streaming velocities using synchronized PIV technique” *Meas. Sci Technol.*, 18, 1811-1817, 2007.

